Tumor recurrence versus treatment effects in glioma

A comparative study of three dimensional pseudo-continuous arterial spin labeling and dynamic susceptibility contrast imaging

Qian Xu, MD[a,b], Qi Liu, MD[b], Haitao Ge, PhD[c], Xinting Ge, PhD[c], Jiangfen Wu, MS[d], Jianxun Qu, PhD[d], Kai Xu, MD, PhD[a,b,*]

Abstract

Background: Gliomas constitute over 90% of primary brain tumors. Accurate identification of glioma recurrence and treatment effects is important, as it can help determine whether to continue with standard adjuvant chemotherapy or to switch to a second-line therapy for recurrence. Our purpose is to compare three dimensional pseudo-continuous arterial spin labeling (3D-pcASL) technique and dynamic susceptibility contrast perfusion magnetic resonance imaging (DSC-MRI) for differentiation tumor recurrence from treatment-related effects in gliomas.

Methods: Twenty-nine patients with gliomas previously who showed enlarged, contrast-enhancing lesions within the radiation field after surgery and concurrent chemoradiotherapy (CCRT) were assessed with 3D-pcASL and DSC-MRI. These patients were classified into 2 groups, tumor recurrence group (n=17) and treatment effects group (n=12), based on pathologic analysis or clinical-radiologic follow-up. The perfusion imaging quality was assessed using a 3-point scale (1=poor imaging, 2=moderate imaging, and 3=good imaging). Comparison for perfusion imaging-quality score between the 2 techniques was performed with Wilcoxon one-sample test. Quantitative analyses were performed between the 2 groups with cerebral blood flow values (ASL-CBF), relative cerebral blood flow values (ASL-rCBF, DSC-rCBF), and relative cerebral blood volume values (DSC-rCBV) using Wilcoxon one-sample test. The intra-class correlation coefficient (ICC) statistics were calculated for testing intrareader variability in regions of interest (ROIs) measurement of all perfusion parameters.

Results: The imaging-quality score of 3D-pcASL was higher than that of DSC-MRI ($P=.01$). The perfusion parameters between tumor recurrence group and treatment effects group had statistically significant differences. There was a significant correlation between ASL-rCBF and DSC-rCBF values ($r=0.803$), between ASL-rCBF and DSC-rCBV values ($r=0.763$), and between DSC-rCBF and DSC-rCBV ($r=0.907$). A receiver operating characteristic (ROC) curve analysis was performed for significant results of perfusion parameters between the 2 groups. Using a cutoff value of 1.110, ASL-rCBF showed the maximum area under the ROC curve (AUC). However, there were no significant differences among different AUCs. The ICC demonstrated excellent agreement for ROIs measurements of ASL-CBF (ICC=0.9636), dynamic susceptibility contrast- cerebral blood flow (DSC-CBF) (ICC=0.8508), and dynamic susceptibility contrast-cerebral blood volume (DSC-CBV) (ICC=0.8543).

Conclusion: 3D-pcASL is an alternative perfusion method to DSC-MRI for the differentiation between tumor recurrence and treatment effects in gliomas. 3D-pcASL is noninvasive and shows fewer susceptibility artifacts than DSC-MRI.

Abbreviations: 3D-pcASL = three dimensional pseudo-continuous arterial spin labeling, AIF = arterial input function, ATT = arterial transit time, AUC = the area under the ROC curve, BBB = blood brain barrier, CBF = cerebral blood flow, CCRT = concurrent chemoradiotherapy, DN = dentate nucleus, DSC-MRI = dynamic susceptibility contrast perfusion magnetic resonance imaging, DWI = diffusion weighted imaging, FLAIR = fluid attenuation inversion recovery imaging, FSE = fast spin echo, GBCA = gadolinium-based contrast agent, Gd-DTPA = gadopentetate dimeglumine, GRE EPI = gradient-echo echo-planar imaging, MRI = magnetic resonance imaging, PLD = post-label delay, rCBF = relative cerebral blood flow, rCBV = relative cerebral blood volume, ROC = receiver operating characteristic, ROIs = regions of interest, SNR = signal-to-noise ratio, SVD = singular value decomposition, T1WI = T1-weighted imaging, T2WI = T2-weighted imaging, TMZ = temozolomide.

Keywords: 3D-pcASL, DSC-MRI, glioma, magnetic resonance imaging, recurrence, treatment effects

---

[a] The First School of Clinical Medicine, Nanjing Medical University, [b] Department of Radiology, Affiliated Hospital of Xuzhou Medical University, [c] Department of Medical Imaging, Xuzhou Medical University, [d] GE Healthcare, Shanghai, China.

* Correspondence: Kai Xu, The First School of Clinical Medicine, Nanjing Medical University, 300 Guangzhou Road, Nanjing, Jiangsu, 210029, China; Department of Radiology, Affiliated Hospital of Xuzhou Medical University, No. 99 Huaihai West Road, Xuzhou, Jiangsu, 221002, China (e-mail: xukaixz@126.com).

1. Introduction

Gliomas constitute over 90% of primary brain tumors diagnosed after the second decade of life.[1] Most patients with gliomas undergo surgical resection followed by concurrent chemo-radiotherapy (CCRT) with temozolomide (TMZ).[2] Patients may develop new or enlarged contrast-enhancing lesions in routine follow-up imaging, which might be induced by tumor recurrence or treatment effects. Treatment effects likely incorporate 2 pathological processes: "pseudo-progression," reflecting subacute and often transient injury (several weeks to months), and "radiation necrosis," reflecting later and more permanent damage (months to several years).[3] However, both of pseudoprogression and radiation necrosis are radiation-induced injuries and irrelevant to tumor recurrence. Accurate identification of tumor recurrence and treatment effects is important, as it can help determine whether to continue with standard adjuvant chemotherapy or to switch to a second-line therapy for recurrence.[4] Although brain tissue pathological examination is the gold standard for the differentiation, invasive approach, occurrence of sampling errors and significant cost limit its wide use. As a feasible and noninvasive method, magnetic resonance imaging (MRI) is now the standard neuroimaging modality in the assessment of treatment response in gliomas.[5] However, conventional MRI is not reliable to distinguish between tumor recurrence and treatment effects, as both of them can cause destruction of the blood brain barrier (BBB), leading to heterogeneous enhancement and T2/FLAIR peritumoral hyperintensity.[6,7]

Angiogenesis is a major feature of brain tumors,[8] and is reported to determine blood flow, metabolism, and growth rate in an irradiated tumor bed.[9] Dynamic susceptibility contrast MR imaging (DSC-MRI), as a surrogate maker for angiogenesis, can be used to evaluate glioma treatment response for differentiating tumor recurrence from radiation necrosis or pseudo-progression.[10–12] However, DSC-MRI needs the introduction of contrast agent and is on the basis of gadolinium-based contrast agent (GBCA) remaining within intravascular space, and violation of this could cause leakage effects,[13] which is especially common in postoperative brain glioma and may confound cerebral blood volume (CBV) and cerebral blood flow (CBF) measurements. Arterial spin labeling (ASL) is a noninvasive MR perfusion technique to quantify CBF. It labeled arterial blood water as an endogenous contrast medium without exogenous injection of contrast agent.[14] Three dimensional pseudo-continuous ASL (3D-pcASL) is a relatively newer technique with rapid 3D acquisition techniques and improved signal-to-noise ratio (SNR) than conventional ASL methods.[15] Previous researches[16–18] have shown the application of ASL on the assessment of primary brain tumors and ischemic stroke.

The purpose of this study aims to compare 3D-pcASL and DSC-MRI derived parameters on their differential capacity between tumor recurrence and treatment-related effects in gliomas following CCRT with TMZ and to evaluate diagnostic ability of the quantitative pharmacokinetic parameter-CBF obtained at 3D-pcASL MR imaging.

2. Material and methods

Approval for this prospective study was obtained from the institutional ethics committee of affiliated hospital of Xuzhou Medical University and written informed consent was obtained from all patients.

2.1. Patient selection

Seventy patients with a new diagnosis of glioma who had undergone surgery and CCRT between June 2014 and October 2016 were enrolled in this prospective study. The inclusion criteria included: the patients had pathologically confirmed glioma according to World Health Organization criteria; had undergone surgery and standard CCRT with TMZ; had undergone baseline CT or MR imaging performed with contrast enhancement within 48 hours after surgery but before subsequent CCRT; had a newly appeared or enlarged enhancing lesion (defined as a bi-dimensionally enhanced lesion with 2 perpendicular diameters of at least 10 mm on MR images) within the radiation field; standard MR scanning protocol, including T1-weighted imaging (T1WI), T2-weighted imaging (T2WI), diffusion weighted imaging (DWI), fluid attenuation inversion recovery (FLAIR) imaging, 3D-pcASL and DSC imaging were performed at an interval of at least every 3 months after CCRT; pathologic diagnosis or subsequent clinical-radiologic follow-up were available for the final diagnosis. We exclude 33 patients in whom no newly appeared or enlarged enhancing lesions were detected, 5 patients without the final diagnosis and 3 patients with severe motion artifacts affecting the visualization of perfusion imaging.

As a result, a total of 29 patients (17 men and 12 women; mean age $\pm$ SD, 47 $\pm$ 11 years) with initial diagnoses of gliomas with grades II (n = 11), III (n = 9), or IV (n = 9) were included and were confirmed to have tumor recurrence (n = 17) and treatment-related effects (n = 12) according to surgical pathology (n = 12) or the response assessment in neuro-oncology criteria[5] (n = 17) during the follow-up (no less than 6 months). The clinical data and reoperative pathology or follow-up of 29 patients were listed in Table 1.

2.2. MR imaging

For each patient, after the completion of CCRT with TMZ, MR imaging was performed on a 3T whole-body scanner (Discovery 750w, GE Healthcare, Milwaukee, Wisconsin) with 3T GEM head and neck unit (HNU) coil. The imaging protocol included precontrast T1WI (TR/TE = 2952.6 ms/24 ms; matrix = 320 × 224; NEX = 2; slice thickness/slice gap = 6 mm/1.5 mm), Propeller T2WI (TR/TE = 4733 ms/100 ms; bandwidth = 62.5; frequency = 416; echo train length = 32; NEX = 1.5; slice thickness/slice gap = 6 mm/1.5 mm), DWI (TR = 4880 ms; matrix = 130 × 160; NEX = 1; slice thickness/slice gap = 6 mm/1.5 mm), FLAIR imaging (TR/TE = 9000 ms/95 ms; matrix = 256 × 256; NEX = 1; slice thickness/slice gap = 6 mm/1.5 mm), 3D-pcASL, and DSC perfusion imaging.

ASL was performed with pseudo-continuous labeling, background suppression, and a 3D stack of spirals fast spin echo (FSE) imaging sequence. The parameters were as follows: TR/TE = 4640/10.7 ms, NEX = 3, bandwidth = 62.5, post-label delay (PLD) time = 1525 ms, field of view = 24 cm × 24 cm, slice thickness = 4 mm, number of slices = 36, scan time of 4 minutes and 29 seconds. DSC was acquired using a T2* weighted gradient-echo echo-planar imaging (GRE EPI) sequence and the following parameters: TR/TE = 1800 ms/30 ms, flip angle = 90, NEX = 1, matrix size = 128 × 128, field of view = 24 cm × 24 cm, slice thickness = 5 mm, scan time of 1 minute and 12 seconds. As a result, 40 phases and 20 images from each phase were obtained. During DSC sequence acquisition, gadopentetate dimeglumine (Gd-DTPA, Magnevist, Bayer Schering Pharma, Germany) was injected at a rate of 3 mL/s and a dose of 0.2 mmol/kg.

Table 1

Clinical data and reoperative pathology or follow-up of 29 patients.

Patient No.	Sex	Age (y)	Initial diagnosis (tumor grade)	Reoperation/follow-up (mo)	Final diagnosis
1	M	25	Glioma (II)	Reoperation	TR
2	F	59	Glioma (III)	Follow-up (16)	TR
3	M	52	Glioma (III)	Reoperation	TR
4	M	42	Glioblastoma (IV)	Reoperation	TR
5	F	48	Glioma (II)	Follow-up (6)	TE
6	M	51	Glioma (II)	Follow-up (26)	TE
7	M	48	Glioma (II)	Follow-up (11)	TR
8	F	41	Glioma (II)	Follow-up (22)	TE
9	M	47	Glioblastoma (IV)	Reoperation	TR
10	M	48	Glioma (III)	Reoperation	TR
11	M	56	Glioblastoma (IV)	Follow-up (8)	TR
12	M	61	Glioblastoma (IV)	Reoperation	TR
13	F	61	Glioblastoma (IV)	Follow-up (7)	TR
14	M	62	Glioma (III)	Reoperation	TR
15	F	51	Glioma (II)	Follow-up (16)	TR
16	F	53	Glioma (II)	Reoperation	TE
17	M	29	Glioma (II)	Follow-up (6)	TE
18	F	57	Glioblastoma (IV)	Reoperation	TE
19	F	32	Glioma (II)	Follow-up (8)	TR
20	M	43	Glioma (III)	Follow-up (6)	TE
21	M	53	Glioma (III)	Follow-up (9)	TE
22	M	53	Glioblastoma (IV)	Follow-up (6)	TR
23	F	52	Glioma (II)	Follow-up (12)	TE
24	F	60	Glioma (III)	Follow-up (6)	TR
25	M	41	Glioblastoma (IV)	Follow-up (6)	TR
26	F	33	Glioma (III)	Reoperation	TE
27	F	19	Glioma (II)	Reoperation	TE
28	M	46	Glioblastoma (IV)	Follow-up (7)	TE
29	M	42	Glioma (III)	Reoperation	TR

TE = Treat-related effects, TR = Tumor recurrence.

Subsequently, conventional postcontrast T1WI was acquired with the same imaging parameters as the precontrast acquisition.

2.3. Assessment of perfusion imaging quality

A susceptibility artifact was defined as signal loss close to interfaces between tissues with different magnetic susceptibility. Two neuroradiologists evaluated the imaging quality of the 2 perfusion methods using a 3-point scale (consensus): 1 = poor imaging with severe susceptibility artifacts (maximum diameter >2 cm), 2 = moderate imaging with small susceptibility artifacts (maximum diameter <2 cm), and 3 = good imaging without susceptibility artifacts.

2.4. Assessment of quantitative perfusion parameters

3D-pcASL and DSC MR Images analyses were performed by using GE Advantage Workstation 4.6 and Functool software (GE Healthcare), in which image fusion was accomplished automatically between postcontrast T1WI and parametric maps. The ASL-CBF, DSC-CBF, DSC-CBV maps were obtained using the software programs on the workstation. In DSC perfusion, the brain tissue concentration–time curve was deconvoluted using singular value decomposition (SVD) with a global arterial input function (AIF) retrieved from the middle cerebral artery branches in the hemisphere contralateral to the enhanced lesion. DSC-MRI maps (rCBF and rCBV) were generated by using an established tracer kinetic model applied to first-pass data.[19] Mathematical correction algorithm was performed to compensate for the confounding estimation of leaky regions of severe BBB breakdown lesions.[20]

Regions of interest (ROIs) of the enhanced lesions, range from 42 to 105 mm^2, were manually drawn by 2 board-certified radiologists (with 20 and 6 years of experience in neuroradiological imaging) who were blinded to the clinical diagnosis within the maximum perfusion area on ASL-CBF maps and DSC-MRI maps, and ROIs were copied to the contralateral regions. Relative cerebral blood flow (rCBF) values and relative cerebral blood volume (rCBV) values were then calculated by dividing the value of enhanced lesion ROI by the value of the contralateral brain tissue on ASL-CBF (ASL-rCBF) map, DSC-CBF (DSC-rCBF) map, and DSC-CBV (DSC-rCBV) map.

2.5. Statistical analysis

Comparison of the imaging-quality score between ASL and DSC-MRI was performed by using Wilcoxon one-sample test. ASL-CBF, ASL-rCBF, DSC-rCBF, and DSC-rCBV between the tumor recurrence group and the treatment effects group were compared using Wilcoxon one-sample test. Spearman's nonparametric correlation test was used to evaluate associations between ASL-rCBF and DSC-rCBF, between ASL-rCBF and DSC-rCBV, and between DSC-rCBF and DSC-rCBV. Additionally, a receiver operating characteristic (ROC) curve analysis was performed for each perfusion parameter to determine the optimal cutoff for differentiating tumor recurrence from treatment effects. The area under the ROC curve (AUC) was used to evaluate the ability for the differentiation diagnosis of perfusion parameters. The intra-class correlation coefficient (ICC) was calculated for testing intra-reader agreement for each ROI measurement (0.00–0.20 poor, 0.21–0.40 fair, 0.41–0.60 moderate, 0.61–0.80 good, and 0.81–1.00
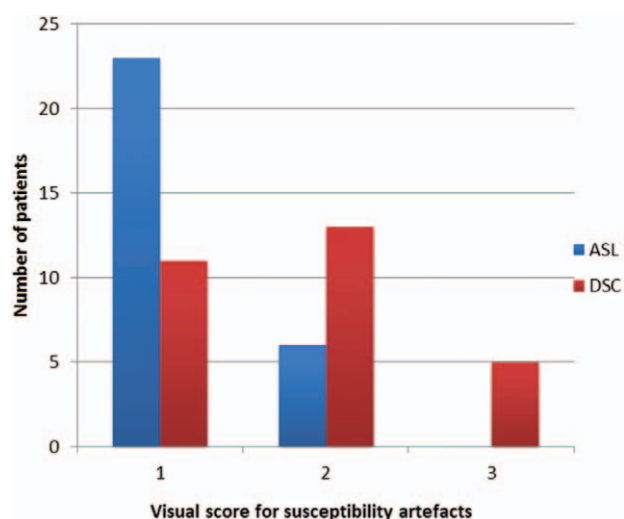
Figure 1. Visual score for susceptibility artifacts for ASL-CBF and DSC-MRI maps (rCBF and rCBV). 1=no susceptibility artifacts, 2=small/moderate (maximum diameter <2 cm) susceptibility artifacts, not affecting imaging evaluation, 3=extensive susceptibility artifacts (maximum diameter >2 cm), deteriorating imaging evaluation. ASL-CBF=arterial spin labeling- cerebral blood flow; DSC-MRI=dynamic susceptibility contrast perfusion magnetic resonance imaging; rCBF=relative cerebral blood flow; rCBV=relative cerebral blood volume.

excellent correlation). Statistical analyses were performed using the SPSS, version 17.0 software package (SPSS Inc., Chicago, IL), and P value <.05 was defined as a statistically significant difference. The agreement between ASL-rCBF and DSC-rCBF measurements was checked using MedCalc version 17.0.4 statistical software (MedCalc Software, Ostend, Belgium), and $P > .05$ was considered to indicate a good agreement between the 2 perfusion methods. Comparisons of different ROC curves were also performed with MedCalc software, and $P < .05$ was considered as significant.

3. Results

3.1. Assessment of perfusion imaging quality in ASL and DSC-MR imaging

ASL-CBF maps obtained a higher imaging-quality score than did DSC-MRI maps (Fig. 1). Susceptibility artifacts were less prominent in ASL-CBF maps (Fig. 2). ASL-CBF maps had an

imaging-quality score of 81, whereas DSC-MRI maps obtained a score of 64. The difference in the scores of imaging quality between the 2 perfusion techniques had a statistically significant difference ($P=.001$).

3.2. Quantitative perfusion analysis in 2 groups

The values of ASL-CBF, ASL-rCBF, DSC-rCBF, and DSC-rCBV in the tumor recurrence group and the treatment effects group were shown in Table 2. There were statistically significant differences in all of the perfusion parameters between the 2 groups (Figs. 3–5). Spearman's correlation coefficients were 0.803 ($P<.001$) between ASL-rCBF and DSC-rCBF, 0.763 ($P<.001$) between ASL-rCBF and DSC-rCBV, and 0.907 between DSC-rCBF and DSC-rCBV ($P<.001$) (Fig. 6). On a Bland-Altman plot analysis, there was no good agreement between ASL-rCBF and DSC-rCBF values ($P=.009$) (Fig. 7).

At ROC curve analysis, the optimal cutoff was an ASL-CBF of 32.325 mL/(100 g min), an ASL-rCBF of 1.110, a DSC-rCBF of 2.364, and a DSC-rCBV of 3.640. By use of a cutoff value of 1.110, ASL-rCBF showed the maximum AUC, however, comparisons of different AUCs found that there were no significant differences among these values ($P>.05$) (Fig. 8, Table 3).

3.3. Intrareader agreement

The ICC test demonstrated excellent agreement for ROIs measurements of ASL-CBF (ICC=0.9636, 95% confidence interval: 0.9240–09827), DSC-CBF (ICC=0.8508, 95% confidence interval: 0.7070–09271), and DSC-CBV (ICC=0.8543, 95% confidence interval: 0.7133–09289).

4. Discussion

Our study has 2 main findings. First, 3D-pcASL can be used in the differentiation between tumor recurrence and treatment effects in the postoperative gliomas, and it is superior to DSC-MRI with insensitivity to susceptibility artifacts, low cost, and avoidance of nephrogenic systemic sclerosis. Second, there is no difference in the diagnostic performance of ASL and DSC-MRI for the differentiation between tumor recurrence and treatment effect.

As a promising noninvasive MR perfusion technique with excellent intra- and interscanner reliability and reproducibility,[15] ASL has been widely used in the evaluation of acute
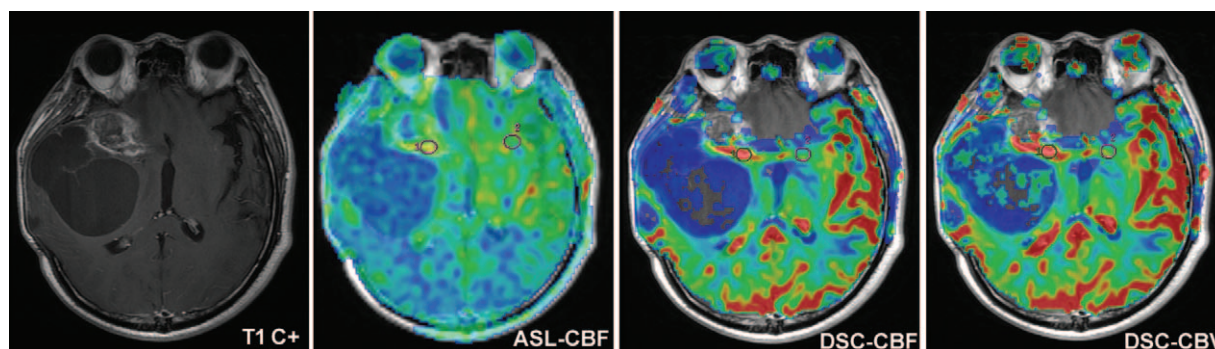
Figure 2. A 42-year-old man with postoperative grade III glioma followed by CCRT with TMZ. Susceptibility artifact was prominent on DSC-MRI maps (rCBF and rCBV) but not on ASL-CBF map. ASL-CBF=arterial spin labeling- cerebral blood flow, CCRT=concurrent chemoradiotherapy, DSC-MRI=dynamic susceptibility contrast perfusion magnetic resonance imaging, rCBF=relative cerebral blood flow, rCBV=relative cerebral blood volume, TMZ=temozolomide.

Parameter	Tumor recurrence	Treatment effect	P value
ASL-CBF (mL/min/100 g)	72.88 ± 42.82	36.81 ± 19.78	.017
ASL-rCBF	2.53 ± 2.05	1.01 ± 0.60	.000
DSC-rCBF	4.74 ± 3.63	1.34 ± 1.06	.001
DSC-rCBV	4.62 ± 3.35	1.75 ± 1.17	.003

ASL = arterial spin labeling, CBF = cerebral blood flow, DSC = dynamic susceptibility contrast, rCBF = relative cerebral blood flow, rCBV = relative cerebral blood volume.

ischemic stroke,[16,17] Alzheimer disease,[21] brain tumors,[18,22] and so on. ASL is a technique using the spin labeled arterial blood water within the vessels and can better reflect the nature of blood perfusion. ASL techniques are commonly classified as continuous ASL (CASL), pulsed ASL (PASL), and pseudocontinuous ASL (pcASL). Both of CASL and PASL have been hindered by the requirement of a continuous-mode radio frequency (RF) transmission, low signal to noise ratio (SNR), and limited imaging coverage.[22] The current pcASL technique, with 3D-spiral FSE acquisition instead of 2D EPI acquisition, includes a longer tagging bolus and higher SNR, therefore providing a
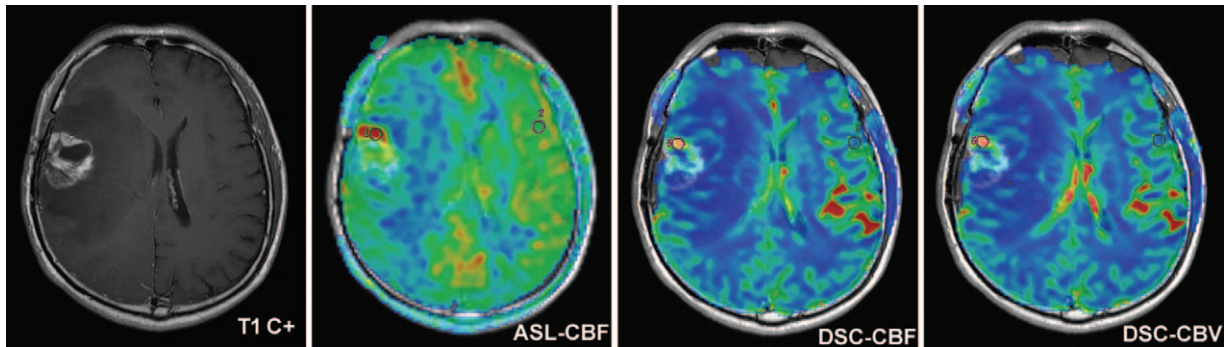

Figure 3. Glioma recurrence in a 62-year-old man with grade III glioma. Contrast-enhanced T1-weighted image illustrated a heterogeneously ring enhanced lesion in the right frontal lobe with a large area of edema 14 months after CCRT. ASL-CBF, DSC-CBF and DSC-CBV maps showed ring-shaped hyperperfusion in the contrast-enhancing lesion, suggesting predominant high-grade tumor recurrence, which was confirmed on histopathology. ASL-CBF = arterial spin labeling-cerebral blood flow, CCRT = concurrent chemoradiotherapy, DSC-CBF = dynamic susceptibility contrast- cerebral blood flow, DSC-CBV = dynamic susceptibility contrast-cerebral blood volume.
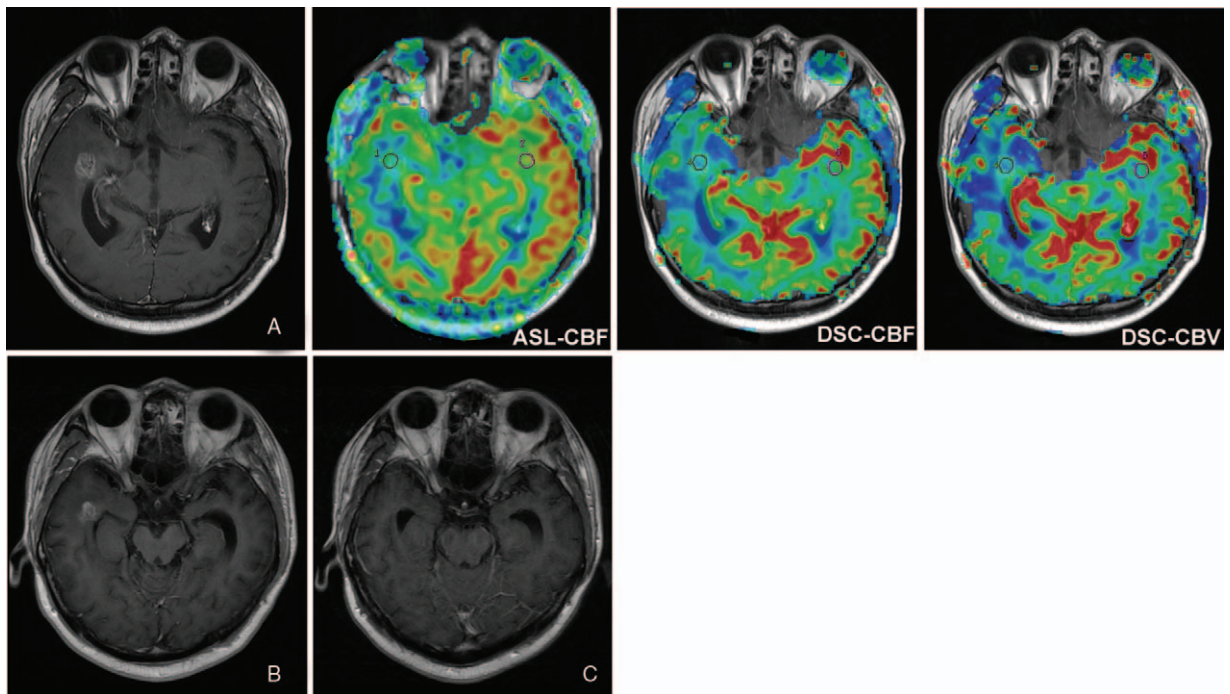
Figure 4. Pseudoprogression in a 29-year-old man with grade II glioma. Contrast-enhanced T1-weighted image obtained 3 months (A), 5 months (B), and 8 months (C) after CCRT. The enhanced lesion in the right temporal lobe around the surgery site gradually disappeared. ASL-CBF, DSC-CBF, and DSC-CBV maps obtained 3 months after CCRT showed iso- or a little hypoperfusion in the contrast-enhancing lesion, suggesting pseudoprogression. ASL-CBF = arterial spin labeling-cerebral blood flow, CCRT = concurrent chemoradiotherapy, DSC-CBF = dynamic susceptibility contrast- cerebral blood flow, DSC-CBV = dynamic susceptibility contrast-cerebral blood volume.
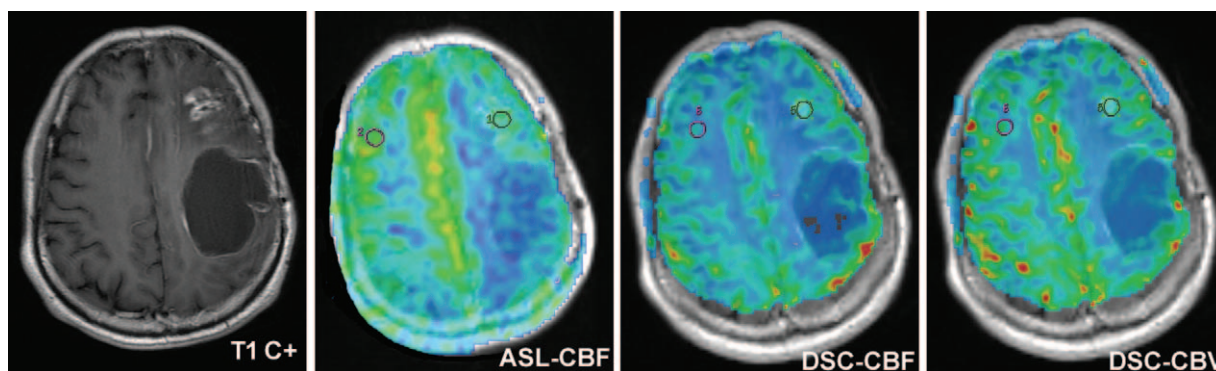
Figure 5. Radiation necrosis in a 53-year-old woman with grade II glioma. Contrast-enhanced T1-weighted image showed a heterogeneously ring enhanced lesion in the left frontal lobe 26 months after CCRT. ASL-CBF, DSC-CBF, and DSC-CBV maps showed iso- or a little hypoperfusion in the contrast-enhancing lesion, highly suggesting radiation-induced necrosis. Reoperative histologic analysis confirmed the diagnosis. ASL-CBF = arterial spin labeling-cerebral blood flow, CCRT = concurrent chemoradiotherapy, DSC-CBF = dynamic susceptibility contrast-cerebral blood flow, DSC-CBV = dynamic susceptibility contrast-cerebral blood volume.
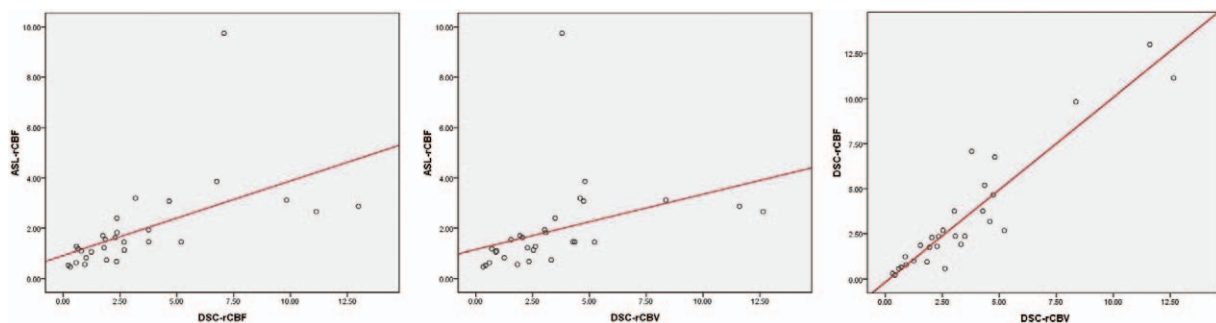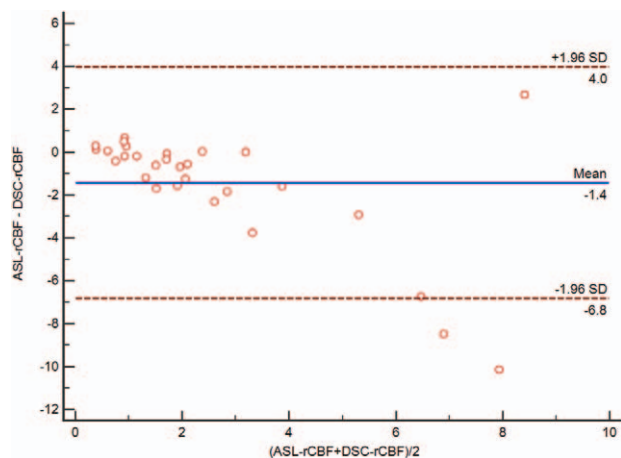

Figure 6. Scatter plot showing ASL-rCBF and DSC-rCBF, ASL-rCBF and DSC-rCBV, as well as DSC-rCBF and DSC-rCBV in all 29 cases. The lines represented linear regression between ASL-rCBF and DSC-rCBF, between ASL-rCBF and DSC-rCBV, and between DSC-rCBF and DSC-rCBV with Spearman correlation coefficient $r = 0.803$, 0.763, and 0.907, respectively. ASL-rCBF = arterial spin labeling-relative cerebral blood flow, DSC-rCBF = dynamic susceptibility contrast-relative cerebral blood flow, DSC-rCBV = dynamic susceptibility contrast-relative cerebral blood volume values.

better balance between tagging efficiency and SNR. In addition, since exogenous GBCA is not acceptable in renal failure patients and could deposit in brain tissue which is associated with increased T1 signal intensity in the dentate nucleus (DN),[23] as

Figure 7. Bland and Altman plot of ASL-rCBF and DSC-rCBF. Dashed line corresponds to 95% limits of agreement. ASL-rCBF = arterial spin labeling-relative cerebral blood flow, DSC-rCBF = dynamic susceptibility contrast-relative cerebral blood flow.

well as the fact that only ASL allows for reproducible absolute quantification of CBF, ASL imaging could be ideal for the long-term follow-up of gliomas during the treatment process.

We have found that the imaging quality of 3D-pcASL was superior to that of DSC-MRI with significant fewer susceptibility artifacts. The lesions close to bone-air interfaces (such as the skull base) are particularly vulnerable to susceptibility artifacts in DSC imaging. DSC-MRI using GRE-EPI acquisition instead of FSE acquisition could explain the more susceptibility artifacts seen in DSC-MRI than in 3D-pcASL imaging in our research.[24] Additionally, old hemorrhage, hemosiderin and iron salt deposition, gliosis and extravasation of contrast media within or around the operation site result in the inhomogeneity of the magnetic field, thus affect the imaging quality of DSC-MRI. However, the wide use of 3D-pcASL is still limited in some aspects. Firstly, 3D-pcASL has a relatively low SNR compared with DSC-MRI. Secondly, it provides only one perfusion parameter-CBF. Thirdly, the scan time of 3D-pcASL (4 minutes and 29 seconds) is longer than DSC-MRI (1 minute and 12 second) and ASL is not suitable for some emergencies.

MR perfusion imaging exploits the neoangiogenic properties of proliferating gliomas, and is able to identify areas of high-grade tumor with high accuracy.[25] High levels of angiogenesis and increasing blood flow are reflected in the perfusion imaging as an increase of perfusion parameter values, while treatment-related changes increase vascular permeability without
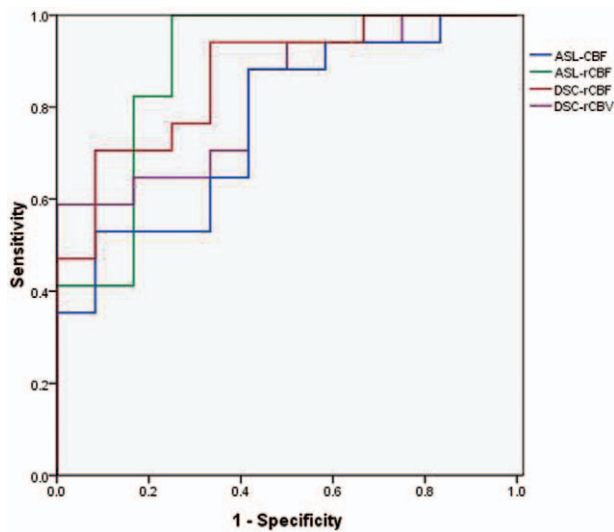
Figure 8. ROC curves of ASL-CBF, ASL-rCBF, DSC-rCBF, and DSC-rCBV for the differentiation between tumor recurrence and treatment effects. ASL-rCBF showed a higher value of AUC than did other perfusion parameters, however, there were no significant differences among the four AUCs. AUC=the area under the ROC curve, ASL-CBF=arterial spin labeling-cerebral blood flow, ASL-rCBF=arterial spin labeling-relative cerebral blood flow, DSC-rCBF= dynamic susceptibility contrast-relative cerebral blood flow, DSC-rCBV= dynamic susceptibility contrast-relative cerebral blood volume.

perfusion imaging, vascular artifacts within the ROI observed in DSC-MRI, leakage effects due to severe BBB disruption in postoperative brain tissues and inhomogeneous materials within the operation area may explain the result.

In this study, quantitative analysis of ASL-rCBF shows the maximum AUC among the 4 parametric AUCs, however, no statistically significant differences were found among them. This indicates there might be no difference in the diagnostic performance of the 2 perfusion methods for differentiating glioma recurrence from treatment effects. Choi's research[30] found ASL improved the diagnostic accuracy of DSC-MRI in differentiating pseudoprogression from early tumor progression and there was no significant difference in the overall diagnostic accuracy of DSC imaging and ASL perfusion MRI. However, a gradient-echo ASL sequence was used in his study, which was more vulnerable to magnetic susceptibility artifacts. Ozsunar's study[31] demonstrated that ASL imaging might more accurately distinguish predominant recurrent high-grade glioma from radiation necrosis compared with DSC-CBV imaging. However, these results were based on the pulsed ASL technique and a single-slice method, thus might introduce selection bias. Additionally, small number of nonrecurrence patients (n=5 for both ASL and DSC imaging) might introduce error into the specificity calculation. Differences between the value of ASL-rCBF and that of DSC-rCBF may be partly due to different calculation models of the 2 perfusion techniques and different diffusion behavior of Gd-DTPA and water molecules; and partly due to the underestimation of CBF in ASL caused by prolonged arterial transit time (ATT) especially in elderly patients.[32]

Our study has several limitations. Firstly, the number of cases used in this study is relatively small. Multicenter clinical trial with larger number of patients is needed to provide the data support and confirm the present results. Secondly, we do not further divide the treatment-related effects groups into pseudoprogression group or radiation necrosis group even though we have observed the 2 different pathological processes, as in our study, we have found the 2 processes overlap in time and differentiating the 2 entities by time of completion of CCRT is somewhat arbitrary,[33] add the fact that pseudoprogression and radiation necrosis may reflect defined time points along a pathologic continuum of radiation damage.[3,7] Thirdly, this study chooses only 1 PLD time (1525 ms) in 3D-pcASL sequence for the differentiation between glioma recurrence and treatment effects. PLD time is essential for CBF measurement as it may lead to an inaccurate estimation of CBF due to differences in the cerebral circulation among individuals. Further research with multi-delay ASL perfusion MRI is needed on the basis of our results.

neoangiogenesis. Studies have reported that rCBV and rCBF calculated out of DSC-MRI can evaluate the blood supply of brain tumors and provide useful information about glioma grading.[22,26] Our results show that there is a close correlation between 3D-pcASL and DSC-MRI in the determination of rCBF in postoperative glioma lesions. This indicates that ASL may provide similar information as DSC perfusion for rCBF measurement, and previous studies have led to the same conclusions.[18,22] Previous studies reported that DSC-rCBV could reliably differentiate tumor true progression from radiation necrosis or pseudoprogression.[10,27–29] According to our results, ASL-rCBF and DSC-rCBF values correlates well with the corresponding DSC-rCBV values, suggesting ASL-rCBF and DSC-rCBF may be as good as DSC-rCBV for the differential diagnosis. However, there is no good agreement between ASL-rCBF and DSC-rCBF values, which is in contradiction with Järnum's research.[18] Different calculation models between the 2 perfusion techniques, the limited PLD time (1525 ms) used in ASL

Table 3

Comparison of AUC, sensitivity, specificity, and accuracy of the perfusion parameters for the differentiation between tumor recurrence and treatment effects.

	ASL-CBF	ASL-rCBF	DSC-rCBF	DSC-rCBV
AUC	0.765 (0.590,0.939)	0.887 (0.752,1.000)	0.868 (0.737,0.998)	0.824 (0.674,0.973)
Sensitivity	0.882 (15/17)	1 (17/17)	0.706 (12/17)	0.588 (10/17)
Specificity	0.583 (7/12)	0.75 (9/12)	0.917 (11/12)	1 (12/12)
Accuracy	0.759 (22/29)	0.897 (26/29)	0.793 (23/29)	0.758 (22/29)
Cut off value	32.325	1.110	2.364	3.640
P-value for ROC curve	.017	.000	.001	.003
P-value for comparison of ROC curves		P>.05		

ASL=arterial spin labeling, AUC=the area under the ROC curve, CBF=cerebral blood flow, DSC=dynamic susceptibility contrast, rCBF=relative cerebral blood flow, rCBV=relative cerebral blood volume, ROC=receiver operating characteristic.

5. Conclusions

In conclusion, our research demonstrates that 3D-pcASL is an alternative perfusion method to DSC-MRI for the differentiation between true progression and treatment-related effects in gliomas. 3D-pcASL is noninvasive and shows fewer susceptibility artifacts than DSC-MRI.

References

[1] Kleihues P, Soylemezoglu F, Schäuble B, et al. Histopathology, classification, and grading of gliomas. Glia 1995;15:211–21.

[2] Stupp R, Mason WP, van den Bent MJ, et al. Radiotherapy plus concomitant and adjuvant temozolomide for glioblastoma. N Engl J Med 2005;352:987–96.

[3] O'Brien BJ, Colen RR. Post-treatment imaging changes in primary brain tumors. Curr Oncol Rep 2014;16:397.

[4] Parvez K, Parvez A, Zadeh G. The diagnosis and treatment of pseudoprogression, radiation necrosis and brain tumor recurrence. Int J Mol Sci 2014;15:11832–46.

[5] Wen PY, Macdonald DR, Reardon DA, et al. Updated response assessment criteria for high-grade gliomas: response assessment in neuro-oncology working group. J Clin Oncol 2010;28:1963–72.

[6] Mullins ME, Barest GD, Schaefer PW, et al. Radiation necrosis versus glioma recurrence: conventional MR imaging clues to diagnosis. AJNR Am J Neuroradiol 2005;26:1967–72.

[7] Linhares P, Carvalho B, Figueiredo R, et al. Early pseudoprogression following chemoradiotherapy in glioblastoma patients: the value of RANO evaluation. J Oncol 2013;2013:690585.

[8] Puduvalli VK, Sawaya R. Antiangiogenesis-therapeutic strategies and clinical implications for brain tumors. J Neurooncol 2000;50:189–200.

[9] Okunieff P, Dols S, Lee J, et al. Angiogenesis determines blood flow, metabolism, growth rate, and ATPase kinetics of tumors growing in an irradiated bed: 31P and 2H nuclear magnetic resonance studies. Cancer Res 1991;51:3289–95.

[10] Barajas RFJr, Chang JS, Segal MR, et al. Differentiation of recurrent glioblastoma multiforme from radiation necrosis after external beam radiation therapy with dynamic susceptibility-weighted contrast-enhanced perfusion MR imaging. Radiology 2009;253:486–96.

[11] Mangla R, Singh G, Ziegelitz D, et al. Changes in relative cerebral blood volume 1 month after radiation-temozolomide therapy can help predict overall survival in patients with glioblastoma. Radiology 2010;256:575–84.

[12] Tsien C, Galbán CJ, Chenevert TL, et al. Parametric response map as an imaging biomarker to distinguish progression from pseudoprogression in high-grade glioma. J Clin Oncol 2010;28:2293–9.

[13] Gahramanov S, Muldoon LL, Li X, et al. Improved perfusion MR imaging assessment of intracerebral tumor blood volume and anti-angiogenic therapy efficacy in a rat model with ferumoxytol. Radiology 2011;261:796–804.

[14] Petcharunpaisan S, Ramalho J, Castillo M. Arterial spin labeling in neuroimaging. World J Radiol 2010;2:384–98.

[15] Wu B, Lou X, Wu X, et al. Intra- and interscanner reliability and reproducibility of 3D whole-brain pseudo-continuous arterial spin-labeling MR perfusion at 3T. J Magn Reson Imaging 2014;39:402–9.

[16] Wang DJ, Alger JR, Qiao JX, et al. The value of arterial spin-labeled perfusion imaging in acute ischemic stroke: comparison with dynamic susceptibility contrast-enhanced MRI. Stroke 2012;43:1018–24.

[17] Huang YC, Liu HL, Lee JD, et al. Comparison of arterial spin labeling and dynamic susceptibility contrast perfusion MRI in patients with acute stroke. PLoS One 2013;8:e69085.

[18] Järnum H, Steffensen EG, Knutsson L, et al. Perfusion MRI of brain tumours: a comparative study of pseudo-continuous arterial spin labelling and dynamic susceptibility contrast imaging. Neuroradiology 2010;52:307–17.

[19] Ostergaard L, Weisskoff RM, Chesler DA, et al. High resolution measurement of cerebral blood flow using intravascular tracer bolus passages. Part I: Mathematical approach and statistical analysis. Magn Reson Med 1996;36:715–25.

[20] Lev MH, Rosen BR. Clinical applications of intracranial perfusion MR imaging. Neuroimaging Clin N Am 1999;9:309–31.

[21] Binnewijzend MA, Kuijer JP, Benedictus MR, et al. Cerebral blood flow measured with 3D pseudocontinuous arterial spin-labeling MR imaging in Alzheimer disease and mild cognitive impairment: a marker for disease severity. Radiology 2013;267:221–30.

[22] Lehmann P, Monet P, de Marco G, et al. A comparative study of perfusion measurement in brain tumours at 3 Tesla MR: Arterial spin labeling versus dynamic susceptibility contrast-enhanced MRI. Eur Neurol 2010;64:21–6.

[23] Bae S, Lee HJ, Han K, et al. Gadolinium deposition in the brain: association with various GBCAs using a generalized additive model. Eur Radiol 2017;27:3353–61.

[24] Wang J, Alsop DC, Li L, et al. Comparison of quantitative perfusion imaging using arterial spin labeling at 1.5 and 4.0 Tesla. Magn Reson Med 2002;48:242–54.

[25] Law M, Yang S, Wang H, et al. Glioma grading: sensitivity, specificity, and predictive values of perfusion MR imaging and proton MR spectroscopic imaging compared with conventional MR imaging. AJNR Am J Neuroradiol 2003;24:1989–98.

[26] Hakyemez B, Erdogan C, Ercan I, et al. High-grade and low-grade gliomas: differentiation by using perfusion MR imaging. Clin Radiol 2005;60:493–502.

[27] Sugahara T, Korogi Y, Tomiguchi S, et al. Posttherapeutic intraaxial brain tumor: the value of perfusion-sensitive contrast-enhanced MR imaging for differentiating tumorrecurrence from nonneoplastic contrast-enhancing tissue. AJNR Am J Neuroradiol 2000;21:901–9.

[28] Gasparetto EL, Pawlak MA, Patel SH, et al. Posttreatment recurrence of malignant brain neoplasm: accuracy of relative cerebral blood volume fraction in discriminating low from high malignant histologic volume fraction. Radiology 2009;250:887–96.

[29] Boxerman JL, Ellingson BM, Jeyapalan S, et al. Longitudinal DSC-MRI for distinguishing tumor recurrence from pseudoprogression in patients with a high-grade glioma. Am J Clin Oncol 2017;40:228–34.

[30] Choi YJ, Kim HS, Jahng GH, et al. Pseudoprogression in patients with glioblastoma: added value of arterial spin labeling to dynamic susceptibility contrast perfusion MR imaging. Acta Radiol 2013; 54:448–54.

[31] Ozsunar Y, Mullins ME, Kwong K, et al. Glioma recurrence versus radiation necrosis? A pilot comparison of arterial spin-labeled, dynamic susceptibility contrast enhanced MRI, and FDG-PET imaging. Acad Radiol 2010;17:282–90.

[32] Wang DJ, Alger JR, Qiao JX, et al. Multi-delay multi-parametric arterial spin-labeled perfusion MRI in acute ischemic stroke—comparison with dynamic susceptibility contrast enhanced perfusion imaging. Neuro-image Clin 2013;3:1–7.

[33] Kruser TJ, Mehta MP, Robins HI. Pseudoprogression after gliomatherapy: acomprehensive review. Expert Rev Neurother 2013;13:389–403.